

Electronic Supplementary Information

Metalated-bipyridine-based porous hybrid polymers with POSS-derived Si-OH groups for synergistic catalytic CO₂ fixation

Yadong Zhang†, Niu Luo†, Jingyu Xu, Ke Liu, Shengqi Zhang, Qinglin Xu, Rui Huang, Zhouyang Long, Minman Tong and Guojian Chen*

School of Chemistry and Materials Science, Jiangsu Key Laboratory of Green Synthetic Chemistry for Functional Materials, Jiangsu Normal University, Xuzhou 221116, China

* Corresponding author: gjchen@jsnu.edu.cn (G. Chen)

† These authors contributed equally to this work

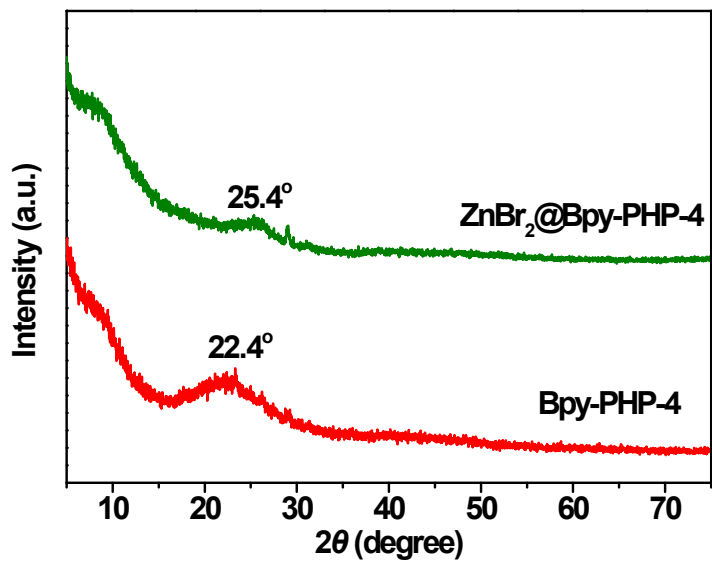


Fig. S1 XRD patterns of Bpy-PHP-4 and $\text{ZnBr}_2@\text{Bpy-PHP-4}$.

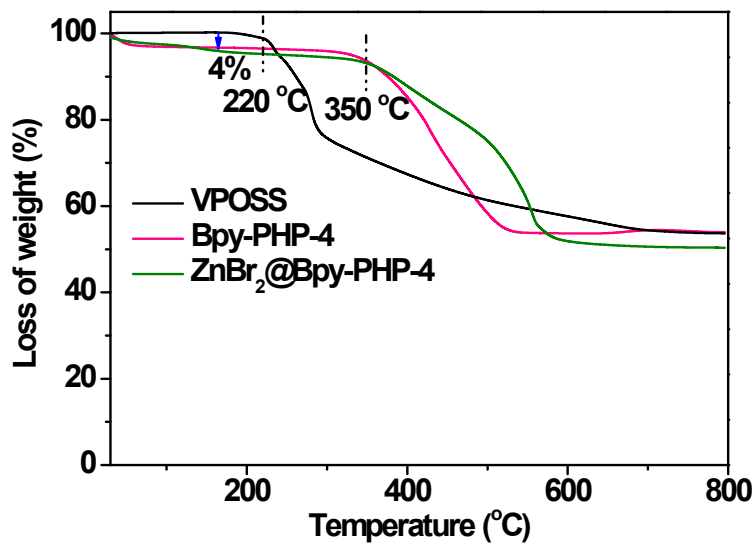


Fig. S2 Thermogravimetric analysis (TGA) curves of VPOSS, Bpy-PHP-4 and $\text{ZnBr}_2@\text{Bpy-PHP-4}$ under air atmosphere.

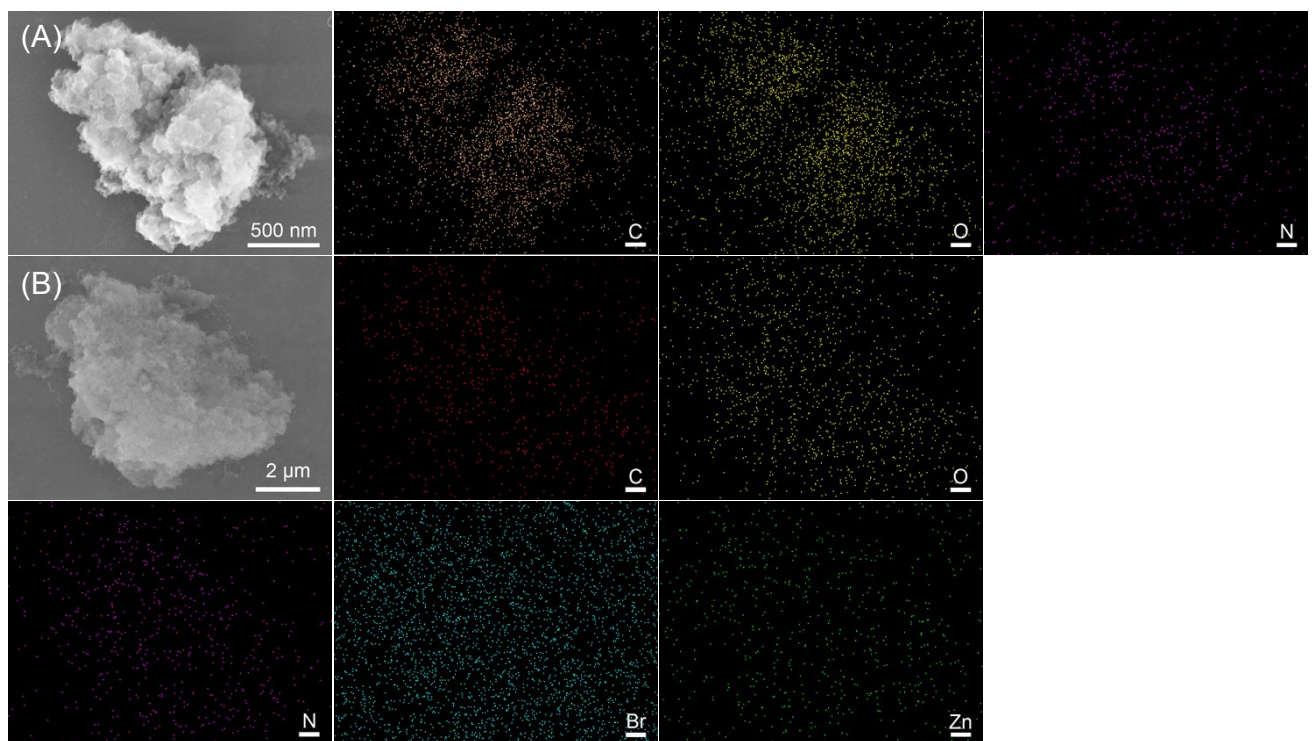


Fig. S3 Energy-dispersive X-ray spectrometry (EDS) elemental mapping images of (A) Bpy-PHP-4 for C, O, N elements and (B) ZnBr₂@Bpy-PHP-4 for C, O, N, Br, Zn elements at the SEM mode.

Table S1 The detailed comparisons of the catalytic activity of ZnBr₂@Bpy-PHP-4 with other metal-based POP and iPOP heterogeneous catalysts in the synthesis of cyclic carbonate from 1,2-epoxyhexane and CO₂.^a

Entry	Catalyst	Co-catalyst ^b	P (MPa)	T (°C)	t (h)	Yield (%)	Ref.
1	Zn-CMP	TBAB	3	120	1	96.1	S1
2	Cr-CMP	TBAB	3	100	2	96.7	S2
3	Bp-Zn@MA	TBAB	1.5	100	1	99	S3
4	Cu/POP-Bpy	TBAB	0.1	50	48	99	S4
5	Co/POP-TPP	TBAB	0.1	29	24	88	S5
6	Py-Zn@MA	none	2	130	12	96	S6
7	PPh ₃ -ILBr-ZnBr ₂ @POPs	none	3	120	1	16	S7
8	Zn-CIF ₂ -C ₂ H ₄	none	2.5	120	4	99	S8
9	SBA-Zn-TPy ⁺ PBr ⁻ _{DMF}	none	1.5	120	4.5	99	S9
10	ZnTPy-BIM4/CNTs-3	none	1.5	120	4	95	S10
11	SYSU-Zn@IL2	none	1	80	24	78	S11
12	POF-Zn ²⁺ -I ⁻	none	1	60	8	82.7	S12
13	Al-CPOP	none	0.1	120	24	15	S13
14	ZnBr₂@Bpy-PHP-4	none	0.1	80	72	99	This work

^a It should be pointed out that different catalysts were evaluated under different conditions (reaction temperature, CO₂ pressure, the amount of substrate/catalyst, solvent, etc.), thus it is difficult to directly compare the activity between different catalytic systems. The represented catalytic activities using yields of the product in Table S1 were obtained under their own optimized conditions, which should be considered in a reasonable comparison; ^b The co-catalyst is tetra-n-butyl-ammonium bromide (TBAB).

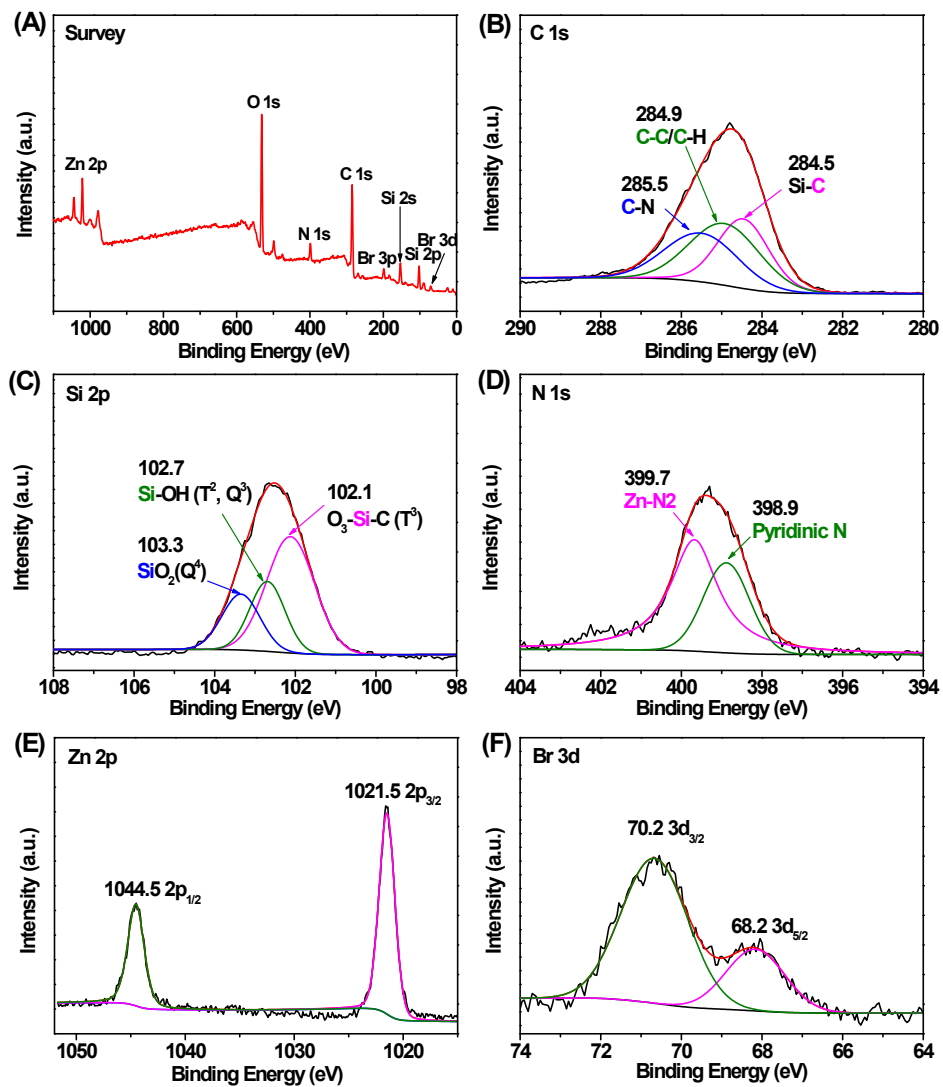


Fig. S4 (A) XPS spectrum survey, (B) C 1s , (C) Si 2p , (D) N 1s, (E) Zn 2p and (F) Br 3d for the reused catalyst $\text{ZnBr}_2@\text{Bpy-PHP-4R}$.

Table S2 The elemental compositions of the fresh catalyst $\text{ZnBr}_2@\text{Bpy-PHP-4}$ and reused $\text{ZnBr}_2@\text{Bpy-PHP-4R}$ detected from XPS.^a

Sample	C (at%)	Si (at%)	O (at%)	N (at%)	Br (at%)	Zn (at%)
The fresh $\text{ZnBr}_2@\text{Bpy-PHP-4}$	49.93	12.57	24.64	6.80	5.26	2.68
The reused $\text{ZnBr}_2@\text{Bpy-PHP-4R}$	50.28	11.72	28.14	6.25	4.65	2.40

^a All elemental compositions were presented by the atomic concentration (at%).

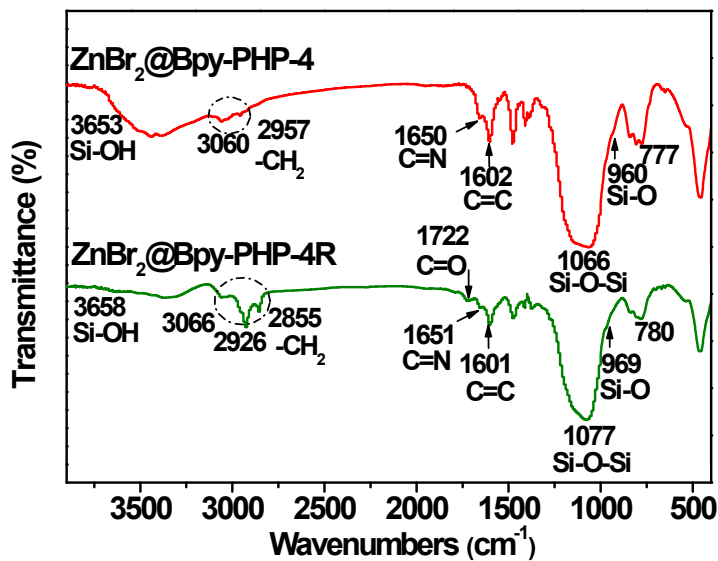


Fig. S5 FTIR spectra of the fresh catalyst $\text{ZnBr}_2\text{@Bpy-PHP-4}$ and the reused catalyst $\text{ZnBr}_2\text{@Bpy-PHP-4R}$.

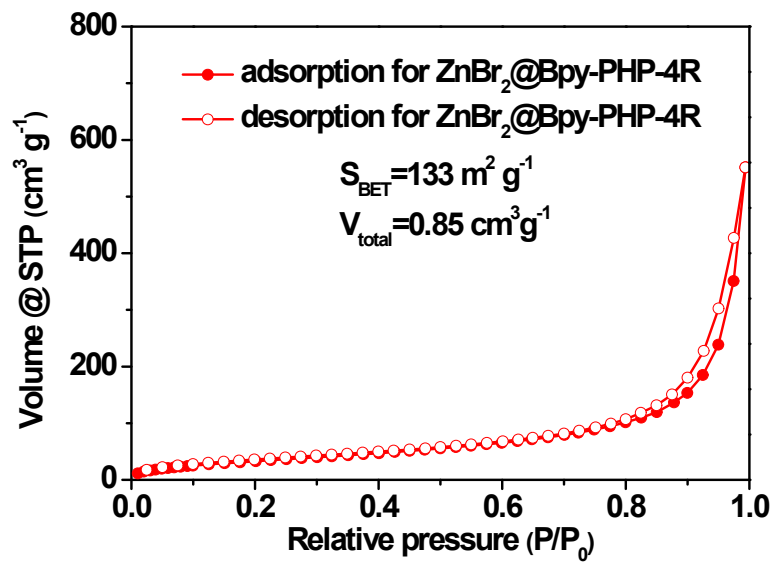


Fig. S6 N_2 -sorption isotherms of the reused catalyst $\text{ZnBr}_2\text{@Bpy-PHP-4R}$.

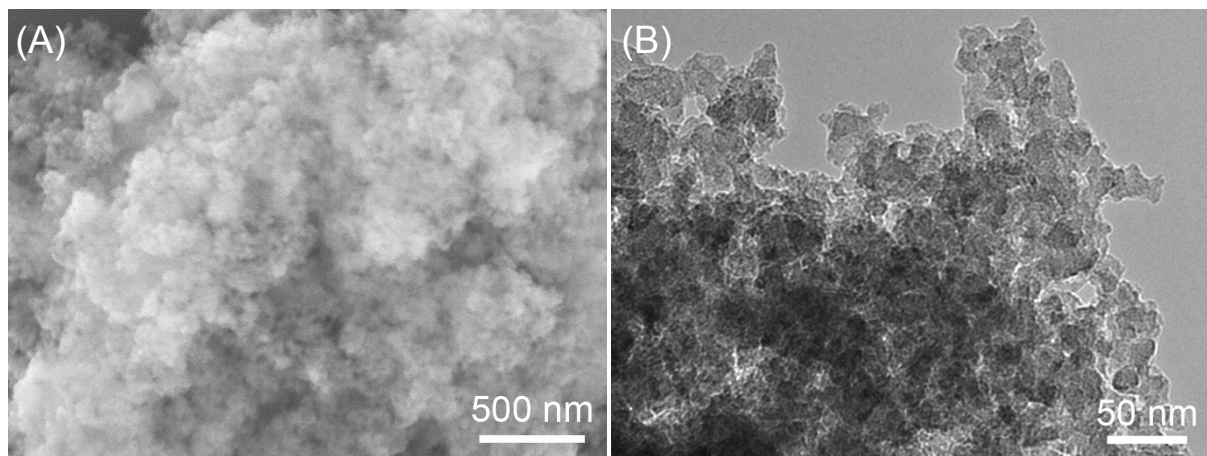


Fig. S7 (A) SEM and (B) TEM images of the reused catalyst $\text{ZnBr}_2@\text{Bpy-PHP-4R}$.

Characterizations for the reused catalyst $\text{ZnBr}_2@\text{Bpy-PHP-4R}$

XPS and FTIR were used to characterize chemical structure and elemental composition of the reused catalyst $\text{ZnBr}_2@\text{Bpy-PHP-4R}$, as shown in Fig. S4, Fig. S5 and Table S2. Compared with the fresh catalyst $\text{ZnBr}_2@\text{Bpy-PHP-4}$, the XPS spectra and elemental compositions for Si, C, N, Zn and Br in the reused $\text{ZnBr}_2@\text{Bpy-PHP-4R}$ have no obvious changes, indicating its well preserved chemical structural composition. The characteristic peaks of reused $\text{ZnBr}_2@\text{Bpy-PHP-4R}$ in FTIR spectrum was almost identical to the fresh catalyst (Fig. S5). However, one new absorption peak was observed at 1722 cm^{-1} and enhanced peaks centered at 2926 cm^{-1} , attributed to the C=O stretching band and $-\text{CH}_2-$ of the cyclic carbonate that slightly adsorbed in the pore of the catalyst. Additionally, $\text{ZnBr}_2@\text{Bpy-PHP-4R}$ was characterized by N_2 -sorption experiment (Fig. S6) plus SEM and TEM (Fig. S7). The S_{BET} and V_{total} values of $\text{ZnBr}_2@\text{Bpy-PHP-4R}$ slightly decrease compared with the fresh one, due to the adsorbed product within the pore of the catalyst. As described in the SEM and TEM images, the porous structure and morphology of $\text{ZnBr}_2@\text{Bpy-PHP-4R}$ was well retained.

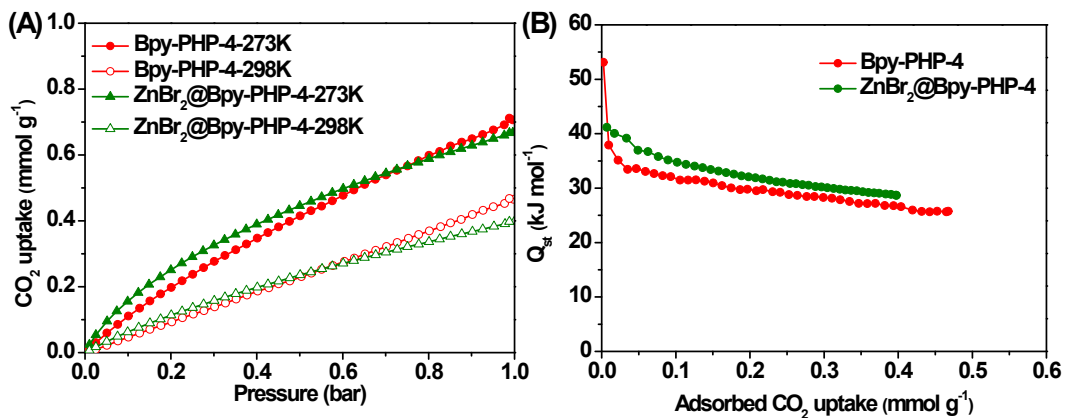


Fig. S8 (A) CO₂ adsorption isotherms of Bpy-PHP-4 and ZnBr₂@Bpy-PHP-4 collected up to 1.0 bar at 273 K and 298 K. (B) The isosteric heat (Q_{st}) plots of CO₂ adsorption for Bpy-PHP-4 and ZnBr₂@Bpy-PHP-4 calculated using the Clausius-Clapeyron equation.

Supplementary ^1H NMR data and spectra for the produced cyclic carbonates

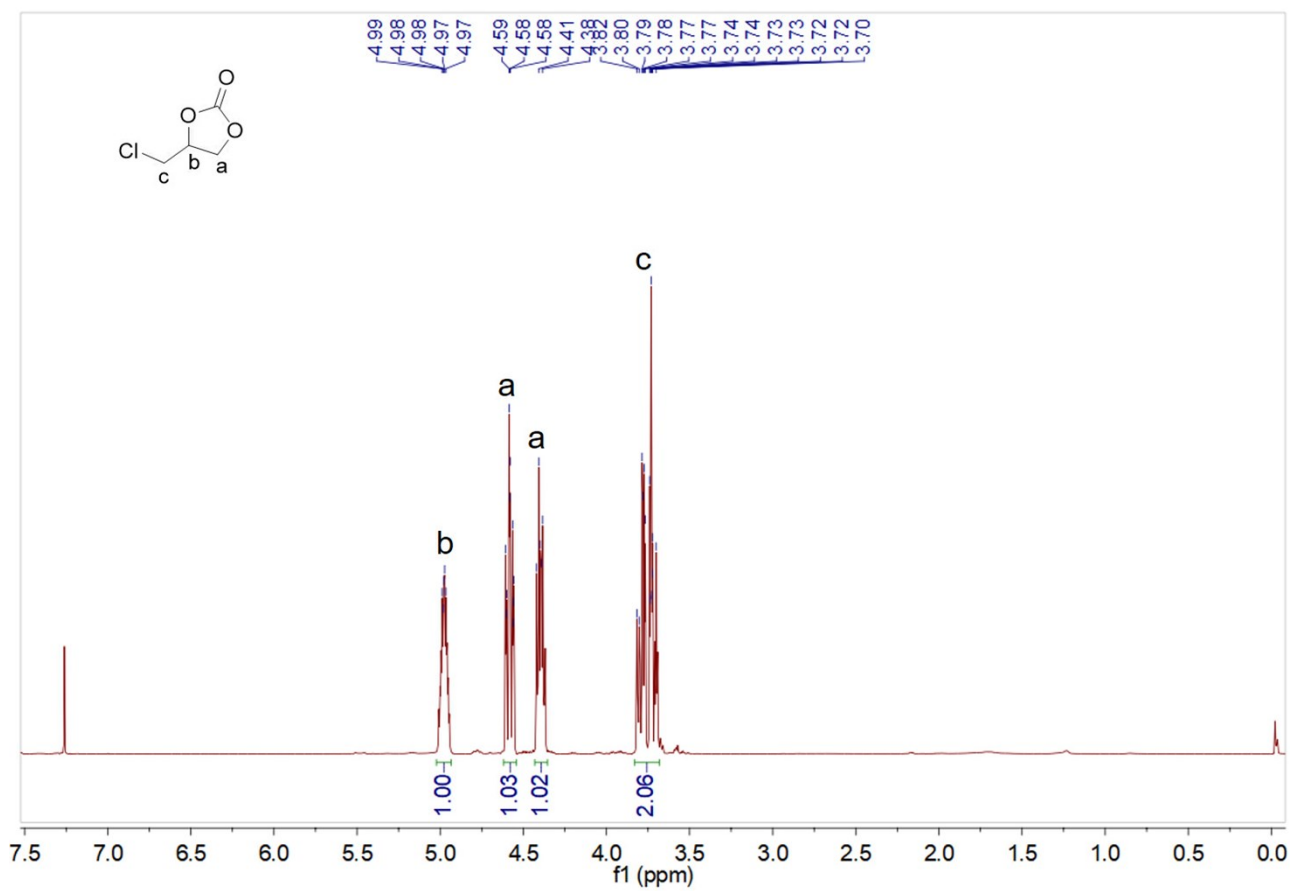


Fig. S9 ^1H NMR spectrum of 4-(chloromethyl)-1,3-dioxolan-2-one (400 MHz, CDCl_3): δ 5.02~4.93 (1H, CH), 4.62~4.54 (1H, CH_2), 4.43~4.35 (1H, CH_2), and 3.83~3.68 ppm (2H, CH_2).

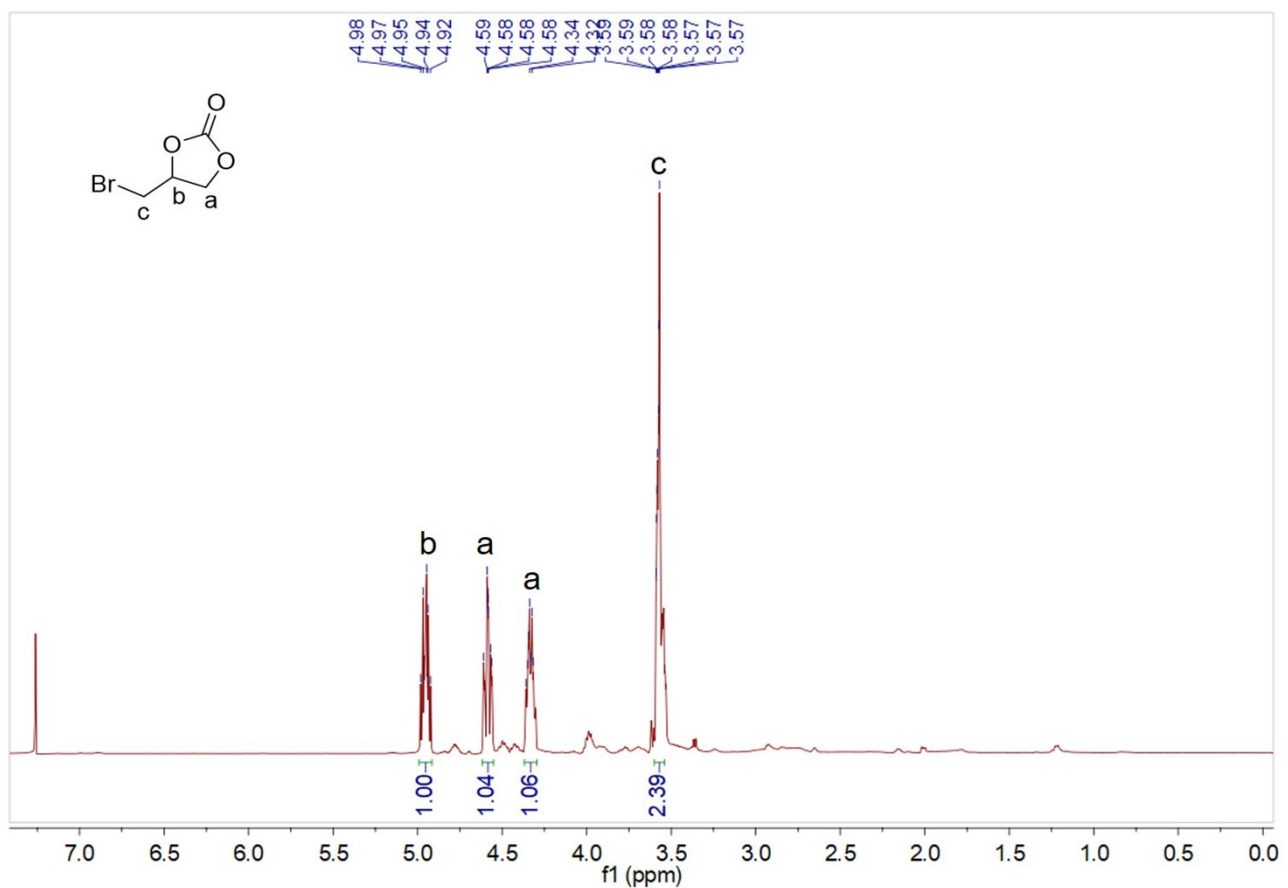


Fig. S10 ^1H NMR spectrum of 4-(bromomethyl)-1,3-dioxolan-2-one (400 MHz, CDCl_3): δ 4.99~4.91 (1H, CH), 4.62~4.55 (1H, CH_2), 4.37~4.30 (1H, CH_2), and 3.60~3.54 ppm (2H, CH_2).

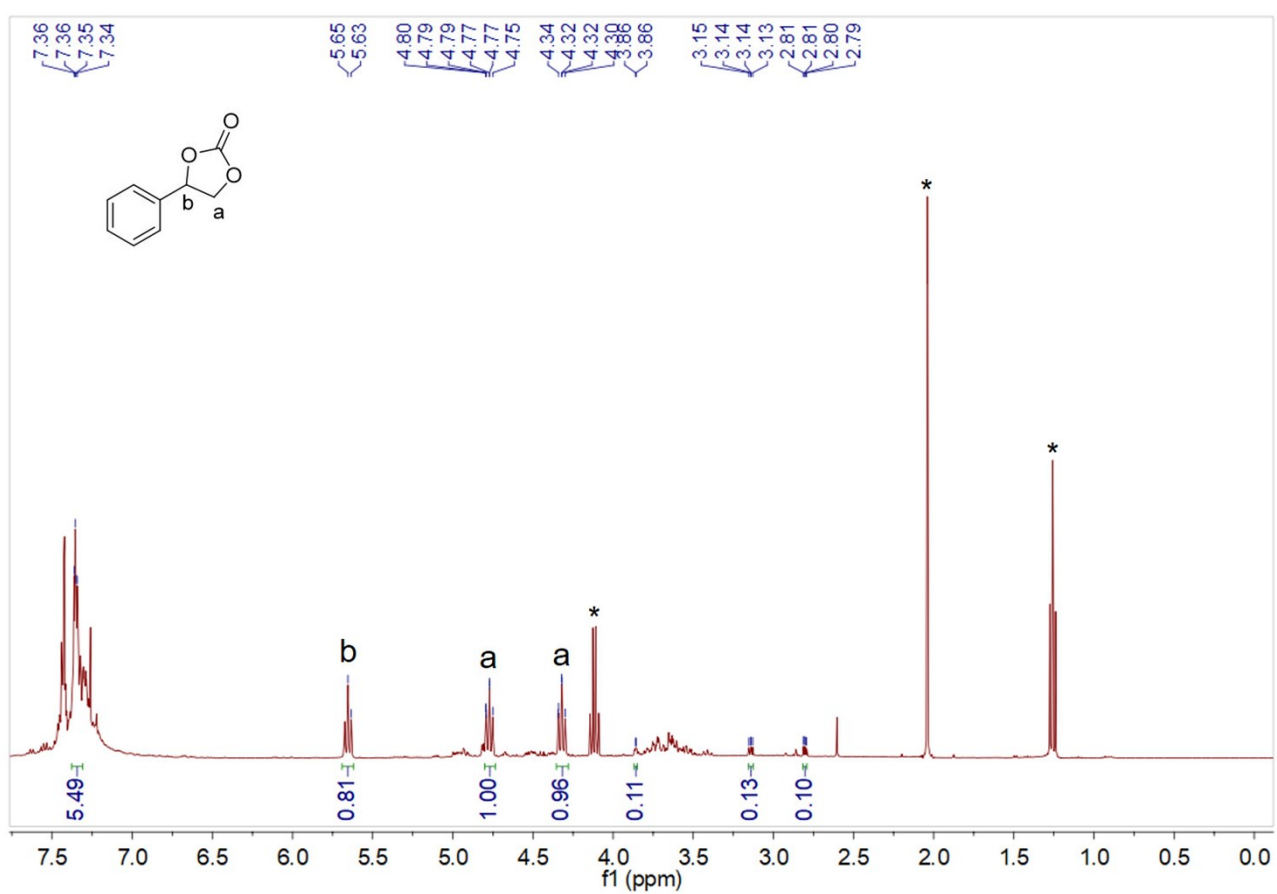


Fig. S11 ^1H NMR spectrum of 4-phenyl-1,3-dioxolan-2-one (400 MHz, CDCl_3): δ 7.35 (5H, CH), 5.64 (1H, CH_2), 4.80~4.74 (1H, CH_2), and 4.35~4.28 ppm (1H, CH_2).

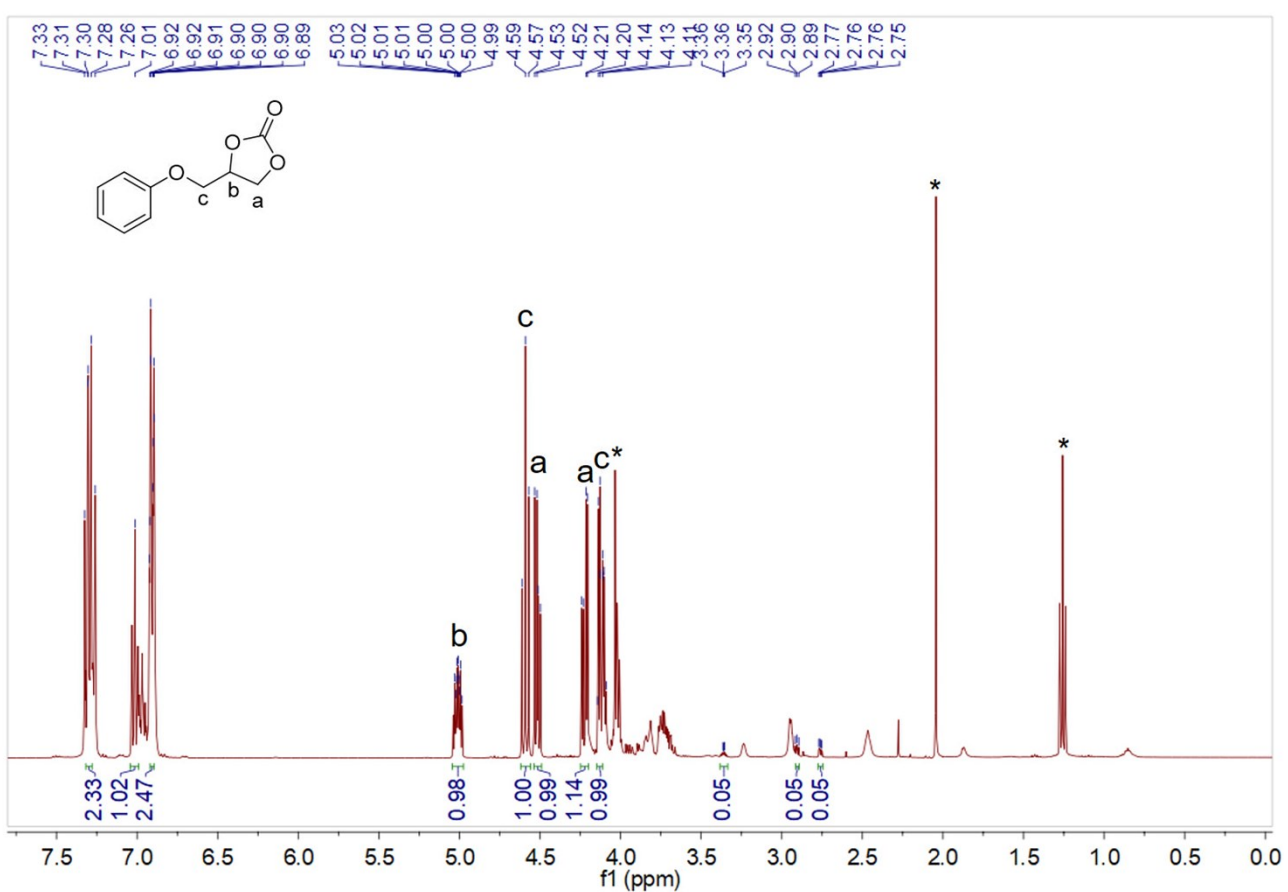


Fig. S12 ^1H NMR spectrum of 4-(phenoxy)methyl)-1,3-dioxolan-2-one (400 MHz, CDCl_3): δ 7.32~7.28 (2H, CH), 7.01 (1H, CH), 6.92~6.89 (2H, CH), 5.04~4.97 (1H, CH), 4.59 (1H, CH_2), 4.52 (1H, CH_2), 4.22 (1H, CH_2), and 4.13 ppm (1H, CH_2).

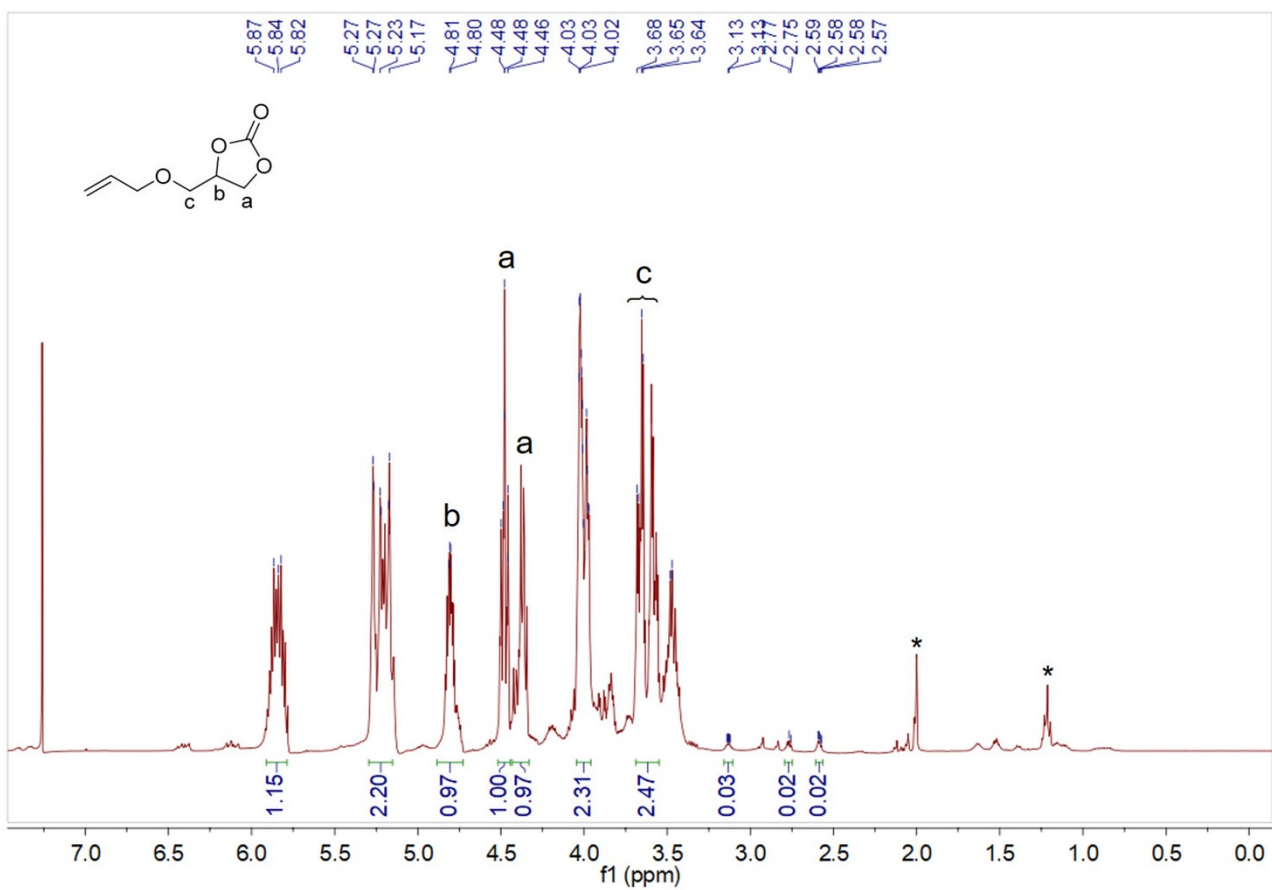


Fig. S13 ^1H NMR spectrum of allyloxymethyl-1,3-dioxolan-2-one (400 MHz, CDCl_3): δ 5.91~5.79 (1H, CH), 5.29~5.15 (2H, CH₂), 4.88~4.73 (1H, CH), 4.52~4.44 (1H, CH₂), 4.38 (1H, CH₂), 4.04~3.96 (2H, CH₂), and 3.66 ppm (2H, CH₂).

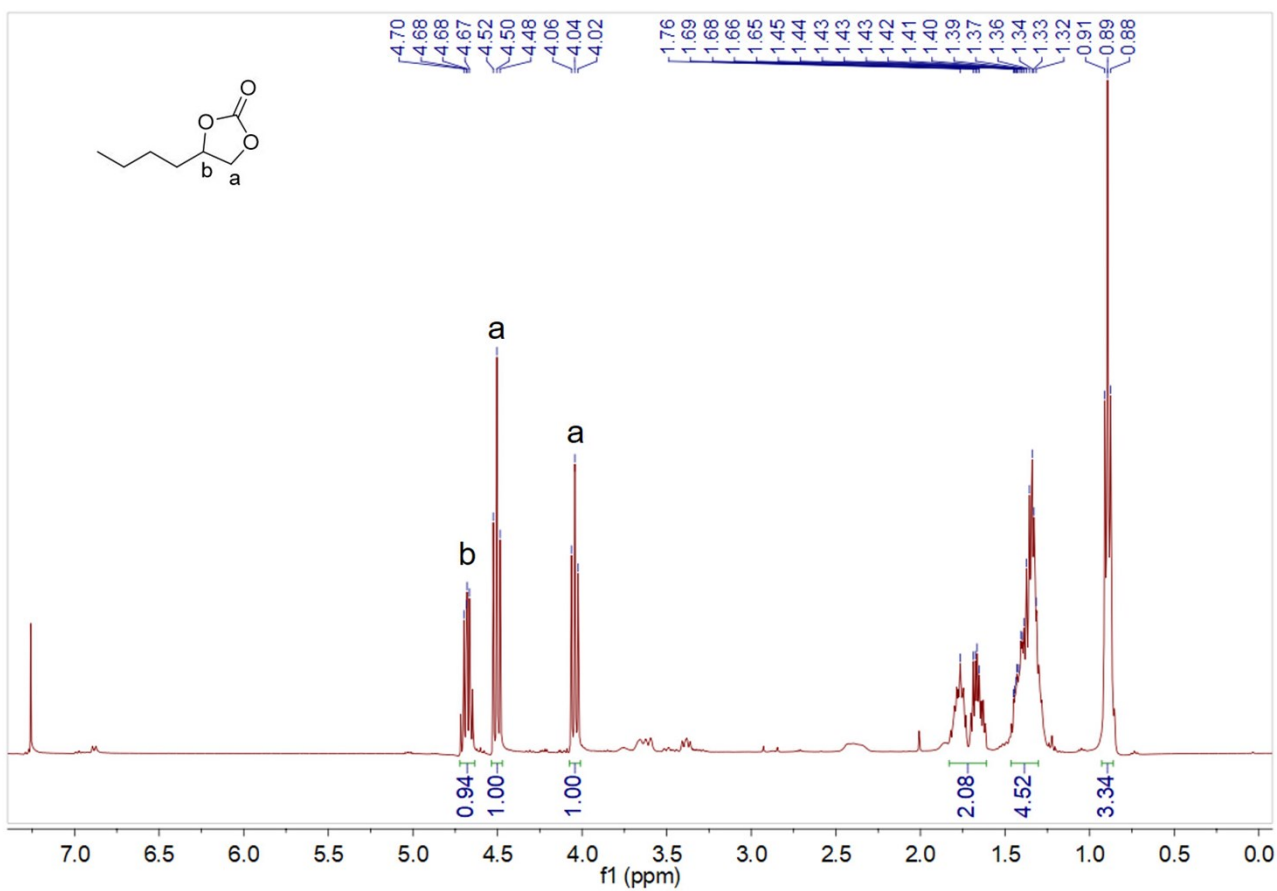


Fig. S14 ^1H NMR spectrum of 4-butyl-1,3-dioxolan-2-one (400 MHz, CDCl_3): δ 4.68 (1H, CH_2), 4.50 (1H, CH_2), 4.04 (1H, CH_2), 1.83~1.61 (2H, CH_2), 1.47~1.30 (4H, CH_2), and 0.89 ppm (3H, CH_3).

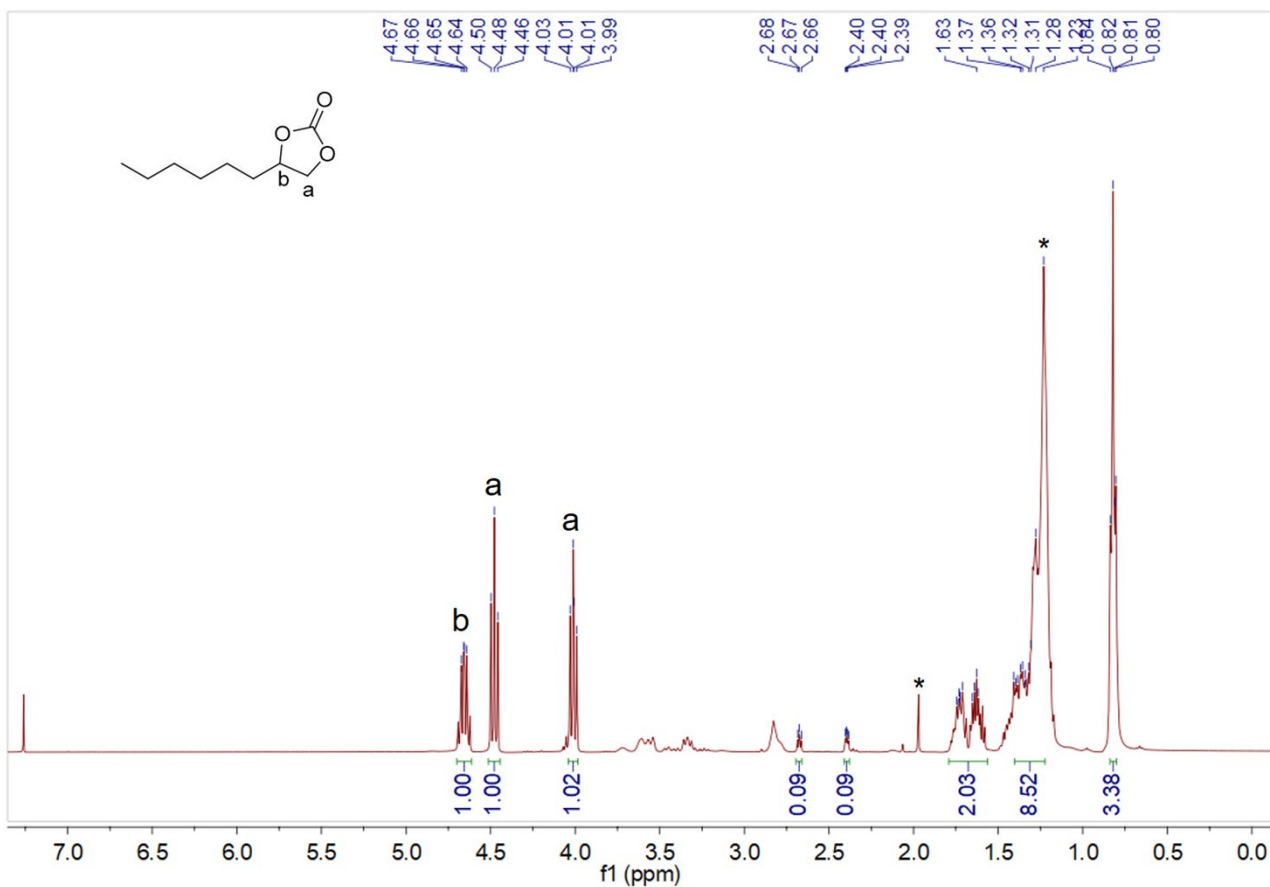


Fig. S15 ^1H NMR spectrum of 4-hexyl-1,3-dioxolan-2-one (400 MHz, CDCl_3): δ 4.66 (1H, CH_2), 4.48 (1H, CH_2), 4.01 (1H, CH_2), 1.79~1.56 (2H, CH_2), 1.40~1.22 (8H, CH_2), and 0.82 ppm (3H, CH_3).

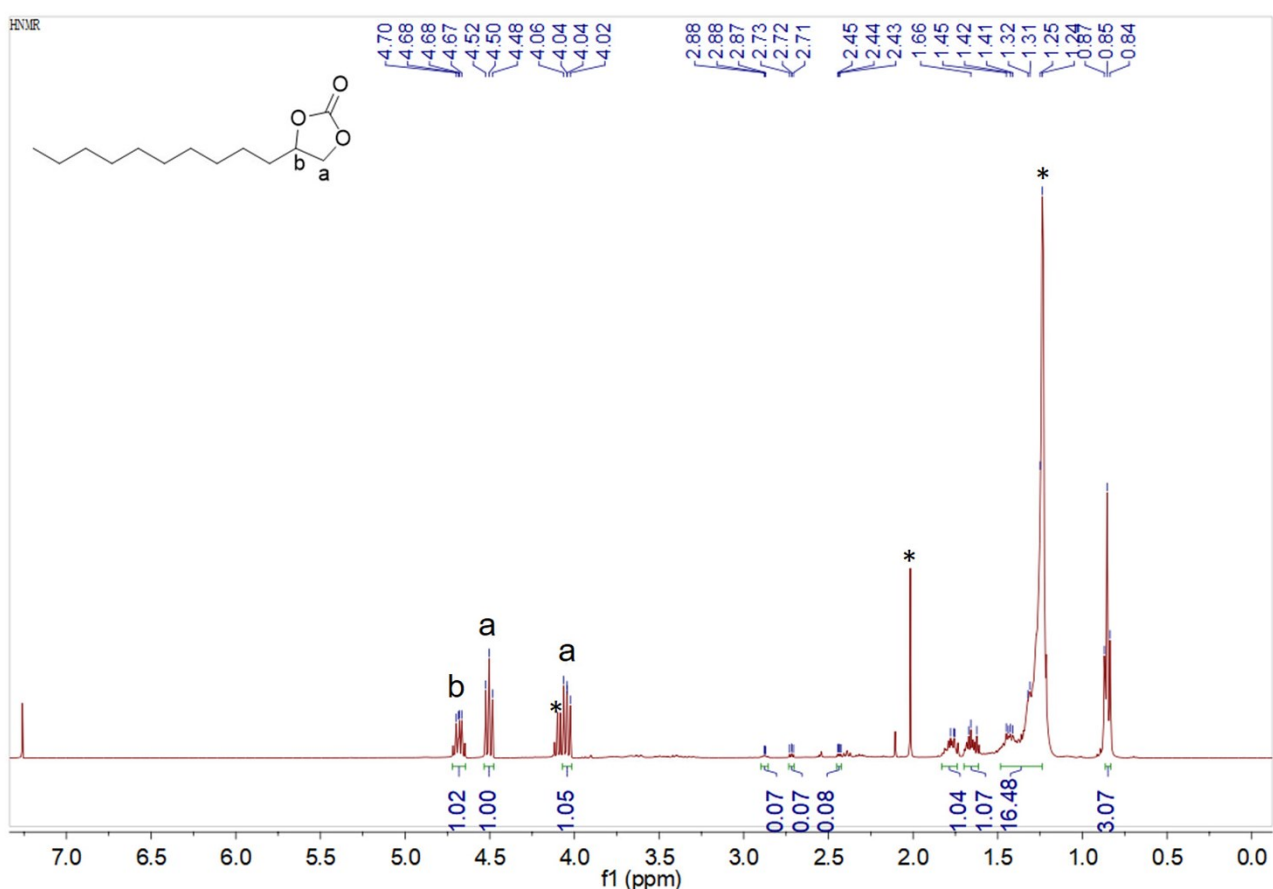


Fig. S16 ^1H NMR spectrum of 4-decyl-1,3-dioxolan-2-one (400 MHz, CDCl_3): δ 4.68 (1H, CH_2), 4.50 (1H, CH_2), 4.04 (1H, CH_2), 1.84~1.74 (2H, CH_2), 1.23 (16H, CH_2), and 0.85 ppm (3H, CH_3).

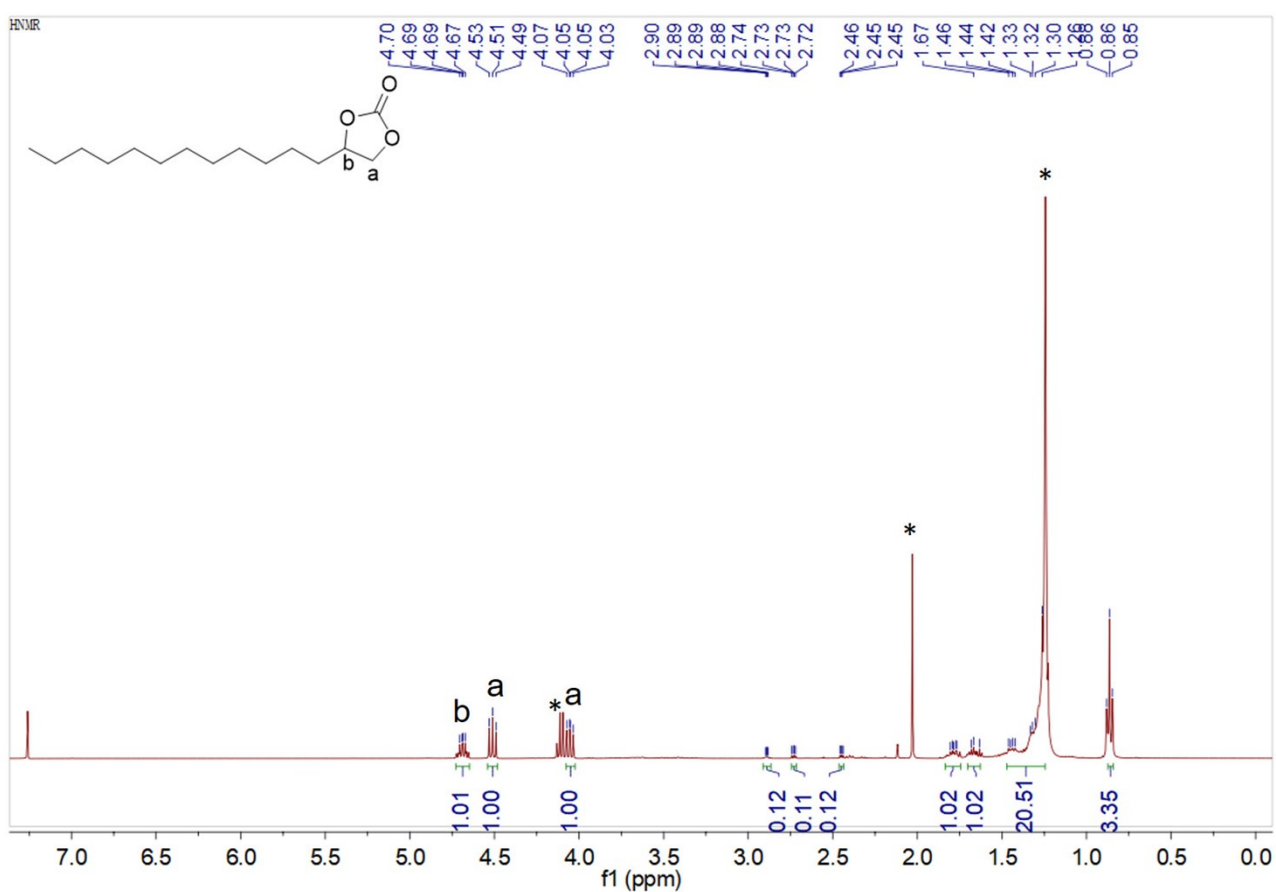


Fig. S17 ^1H NMR spectrum of 4-dodecyl-1,3-dioxolan-2-one (400 MHz, CDCl_3): δ 4.69 (1H, CH_2), 4.54~4.48 (1H, CH_2), 4.05 (1H, CH_2), 1.83~1.74 (2H, CH_2), 1.24 (20H, CH_2), and 0.86 ppm (3H, CH_3).

References

- (S1) Y. Xie, T.-T. Wang, R.-X. Yang, N.-Y. Huang, K. Zou and W.-Q. Deng, *ChemSusChem*, 2014, **7**, 2110-2114.
- (S2) Y. Xie, R.-X. Yang, N.-Y. Huang, H.-J. Luo and W.-Q. Deng, *J. Energy Chem.*, 2014, **23**, 22-28.
- (S3) J. Chen, H. Li, M. Zhong and Q. Yang, *Green Chem.*, 2016, **18**, 6493-6500.
- (S4) Z. Dai, Q. Sun, X. Liu, L. Guo, J. Li, S. Pan, C. Bian, X. Hu, X. Meng, L. Zhao, F. Deng and F.-S. Xiao, *ChemSusChem*, 2017, **10**, 1186-1192.
- (S5) Z. Dai, Q. Sun, X. Liu, C. Bian, Q. Wu, S. Pan, L. Wang, X. Meng, F. Deng and F.-S. Xiao, *J. Catal.*, 2016, **338**, 202-209.
- (S6) H. Li, C. Li, J. Chen, L. Liu and Q. Yang, *Chem. Asian J.*, 2017, **12**, 1095-1103.
- (S7) W. Wang, C. Li, L. Yan, Y. Wang, M. Jiang and Y. Ding, *ACS Catal.*, 2016, **6**, 6091-6100.
- (S8) J. Liu, G. Zhao, O. Cheung, L. Jia, Z. Sun and S. Zhang, *Chem. Eur. J.*, 2019, **25**, 9052-9059.
- (S9) S. Jayakumar, H. Li, L. Tao, C. Li, L. Liu, J. Chen and Q. Yang, *ACS Sustainable Chem. Eng.*, 2018, **6**, 9237-9245.
- (S10) S. Jayakumar, H. Li, J. Chen and Q. Yang, *ACS Appl. Mater. Interfaces*, 2018, **10**, 2546-2555.
- (S11) Y. Chen, R. Luo, Q. Xu, J. Jiang, X. Zhou and H. Ji, *ACS Sustainable Chem. Eng.*, 2018, **6**, 1074-1082.
- (S12) D. Ma, J. Li, K. Liu, B. Li, C. Li and Z. Shi, *Green Chem.*, 2018, **20**, 5285-5291.
- (S13) T.-T. Liu, J. Liang, Y.-B. Huang and R. Cao, *Chem. Commun.*, 2016, **52**, 13288-13291.